REPORT DOCUMENTATION PAGE

1. AGENCY USE ONLY (Leave blank)	2. REPORT DATE 1/96	3. REPORT TYPE AND DATES COVERED Final Report: 6/15/92 - 5/31/95

4. TITLE AND SUBTITLE

(FY91 AASERT) Superconductivity in Low-Temperature Grown III-V Thin Films

5. FUNDING NUMBERS

Grant
~~F49620-92-J-0354~~
61103D
3484/s3

6. AUTHOR(S)

Eicke R. Weber

7. PERFORMING ORGANIZATION NAME(S) AND ADDRESS(ES)

Regents of the University of California
c/o Sponsored Projects Office
336 Sproul Hall
Berkeley, CA 94720-5940

8. PERFORMING ORGANIZATION REPORT NUMBER

AFOSR-TR
96-0059

9. SPONSORING/MONITORING AGENCY NAME(S) AND ADDRESS(ES)

AFOSR ~ NE
Building 410
Bolling AFB DC 20332-6448

10. SPONSORING/MONITORING AGENCY REPORT NUMBER

F49620.92-J-0354

11. SUPPLEMENTARY NOTES

12b. DISTRIBUTION CODE

13. ABSTRACT (Maximum 200 words)

In this AASERT project, two graduate students of the University of California, Berkeley, studied the electronic properties of various low-temperature grown III-V thin films using both optical and electrical characterization techniques. Very early on, the previously found superconductivity effect could be ascribed to inclusions of group-III elements that were not related to the low-temperature growth conditions. The results found here indicate that the anion antisite, As_{Ga}, dominates the properties of LT-GaAs. This finding will allow future improvements in LT-GaAs by designing optimized concentrations of As_{Ga}-related deep levels for specific applications. In LT-AlGaAs, the very deep arsenic antisite level leads to the formation of layers with very high resistivity. In LT-InP and possibly in LT-InAlAs, the energy location of the anion antisite defects prevents the formation of highly resistive, undoped layers. With MCDA we were able to directly prove that LT InP is highly n-type due to P_{In} antisite defects, and to suggest which transitions form the magnetic circular dichroism spectrum for this defect.

14. SUBJECT TERMS

15. NUMBER OF PAGES

16. PRICE CODE
n/a

17. SECURITY CLASSIFICATION OF REPORT n/a	18. SECURITY CLASSIFICATION OF THIS PAGE n/a	19. SECURITY CLASSIFICATION OF ABSTRACT n/a	20. LIMITATION OF ABSTRACT n/a

19960220 028

DTIC QUALITY INSPECTED 1

I. INTRODUCTION

The finding of superconductivity in GaAs with low-temperature grown III-V thin films [1] was found to be due to inclusions of In or Ga in GaAs [2] rather than to the excess As to which it originally was ascribed. Therefore, further work on the superconductivity phenomenon was no longer related to low-temperature grown GaAs, the parent contract of the AASERT award. After consultation with the AFOSR program manager it was decided that the two graduate students supported by the AASERT award were rather to work on other properties of low-temperature grown III-V thin films. The first student, Howard Chang, finished his Masters of Science in May of 1994 with a thesis entitled: "Defect Characterization in LT-AlInAs," the second student, Arti Prasad, will finish her Ph.D. thesis in Spring of 1996. The scientific results of both students will be summarized in the following chapter.

2. INVESTIGATIONS ON LOW-TEMPERATURE GROWN III-V THIN FILMS

During the three years of the AASERT award we have investigated the optical and electrical properties of various novel non-stoichiometric semiconductors. A major emphasis has been placed on GaAs grown via molecular beam epitaxy (MBE) at low substrate temperatures of ~200°C (LT GaAs), due to potential industrial applications as well as to the scientific controversy over the defect which controls both the electrical and optical properties. These studies conclude that the native defect, the arsenic antisite (As_{Ga}), plays a dominant role. Additionally, the continuing study on LT-InP resulted in the observation that the prevailing defect is as well the anion antisite, the phosphorus antisite (P_{In}). Other materials studied were LT $Al_{1-x}Ga_xAs$ which has a higher resistivity than LT GaAs upon annealing and therefore might be more useful in applications, and LT-InAlAs which can be grown lattice matched to InP substrates.

2.1. LT-GaAs

The semi-insulating (SI) properties of annealed GaAs grown at low temperatures (LT GaAs) by molecular beam epitaxy (MBE) are explained by two controversial models still under debate: the "buried Schottky barrier" model [3] and the "arsenic antisite defect" model [4]. The former explains the SI properties in terms of overlapping depletion regions around As precipitates formed upon annealing, while the latter attributes the semi-insulating properties to the residual As_{Ga} defects which pin the Fermi level close to midgap. A key question for the defect model is what are the concentrations of As_{Ga} defects in neutral and positively charged states, $[As_{Ga}^0]$ and $[As_{Ga}^+]$. With the goal of resolving this controversy we measured $[As_{Ga}^0]$ and $[As_{Ga}^+]$ as determined by near-infrared absorption and magnetic circular dichroism of absorption (MCDA),

respectively [5]. In the as-grown state (~200°C) the antisite concentration is ~10^{20} cm^{-3} for the neutral defect and ~10^{18} cm^{-3} for the positive defect. As seen in Figures 1 and 2, the defect concentration decreases significantly for annealed materials, and for samples grown at higher temperatures. However, we find that a high concentration of defects is always present in the LT GaAs studies, with the concentration of As_{Ga}^0 larger than that of As_{Ga}^+ defects. Transmission electron microscopy of the samples shows that the onset of precipitate formation is ~400°C [6]. Significant decrease in the defects' concentration also starts at similar temperatures. Nevertheless, it is clear that $[As_{Ga}^0] > [As_{Ga}^+]$ is maintained during the formation of the As precipitates. This shows that the annealing dynamics is a process of forming As precipitates in the GaAs matrix in which the Fermi level is close to midgap. A near-flatband condition is thus maintained in the process of precipitation with little charge transfer expected between the GaAs matrix and the As precipitates. Thus the semi-insulating properties of LT GaAs are not caused by precipitates, because As_{Ga} defects can well account for the pinning of the Fermi level close to midgap, and hence the semi-insulating properties of the material. Further investigations into this material showed that the change of lattice parameter correlates with the concentration of As_{Ga} (Figure 3), and that As_{Ga} alone can account for the lattice expansion [7]. Also, the total concentration of As_{Ga} has a characteristic second power dependence on the concentration of As_{Ga} in the positive charge state for the material grown at different temperatures (Figure 4). This can be understood provided that V_{Ga} defects are the acceptors responsible for the carrier compensation. This result is consistent with theoretical calculations of defect formation energies. Therefore, our studies indicate that the dominant defects in LT GaAs are the arsenic antisite and the gallium vacancy.

2.2. LT $Al_xGa_{1-x}As$.

From the analysis of defect concentrations we noticed that the behavior of the MCDA spectrum of the arsenic antisite in LT GaAs is quite different from that found in bulk SI GaAs. The spectrum of the bulk material has one negative (0.94 eV) and two positive (1.1 eV and 1.35 eV) bands [9] (Figure 5a). In comparison, the MCDA of LT GaAs has only two observable negative peaks [10] (0.94 eVa nd 1.18 eV) (Figure 5b). MCDA is sensitive to paramagnetic defects; however, high concentrations of diamagnetic defects can also contribute [11]. Magnetic resonance studies on the MCDA peaks (ODMR--Optically Detected Magnetic Resonance) of the bulk spectrum show that the signals are due to As_{Ga}^+ [9]. In LT GaAs the 0.94 eV peak is paramagnetic and comes from As_{Ga}^+ as observed by ODMR and temperature dependence (paramagnetic signal is temperature dependent whereas diamagnetic signal is not), and the 1.18 eV peak is mostly diamagnetic as evidenced by the independence of the MCDA from the temperature [10]. We have suggested that this diamagnetic peak is related to the A1(T2 internal transition associated with the diamagnetic state of the As antisite, As_{Ga}^0. Occurrence of the diamagnetic band in the MCDA is due to the high concentration of As_{Ga}^0, ~10^{20} cm^{-3}. LT $Al_xGa_{1-x}As$ also has such a high concentration of the antisite, and we have observed a similar spectrum. At low Al percentage the MCDA spectrum of LT $Al_xGa_{1-x}As$ has the same features of two negative peaks (Figure 6). As the amount of Al increases the two peaks still exist yet they start to shift to higher energies with the

paramagnetic peak shifting faster than the diamagnetic peak. Eventually the paramagnetic peak merges into the diamagnetic peak (around x=0.2), but a definite shoulder at lower energies is visible. Even the shoulder disappears near x=0.3. For x=0.3 the only MCDA band observed is located at 1.35 eV. Photo quenching studies indicate that these two peaks and eventually the one peak are associated with the As_{Ga} defect. In the past, two models, the internal-transition model [9] and the valence-band-transition model [12], have been proposed to explain the MCDA spectrum of bulk semi-insulating (SI) GaAs. According to Meyer et al., in the internal transition model, the MCDA transitions of As_{Ga}^+ are intra-center from the A1 ground state to the T2 excited states of the defect which are resonant with the conduction band. Because the transitions are internal, they are not expected to be strongly affected by the change in bandgap. The valence-band-transition model proposed by Kaufmann et al. postulates that the two MCDA transitions of bulk GaAs are the hole transitions from the ground As_{Ga}^+ defect to the excited valence band states. If this model is applied to the behavior of As_{Ga}^+ in LT $Al_xGa_{1-x}As$, it would require the valence band to shift with the increasing Al content. Studies done by J. Menidez et al. [13] show that the valence band of $Al_xGa_{1-x}As$ shifts with the Al composition. From our results in LT $Al_xGa_{1-x}As$ the large shift in energy of the paramagnetic MCDA band seems to be in good accord with the shifting valence band. The internal transition model cannot account for the large shift. Thus, this shift is in better agreement with the valence band model. Also, the diamagnetic band in the MCDA spectra shifts slower than the paramagnetic band to higher energies with Al content, which is clearly indicated by the merging of the two spectra (Figure 6). The shift is still slightly larger than expected from the pressure dependence of the internal transition of EL2. However, the deviation is not large enough to make a conclusive statement about this tentatively assigned transition; further studies are needed.

2.3. LT InP.

The success of LT GaAs as a highly resistive buffer layer has inspired researchers to explore the use of LT InP for the same purpose. However experiments showed that LT InP on the contrary is highly n-type conductive [14]. Previously it has been suggested that this might be due to the presence of the P_{In} antisite, but no direct proof was given. We have obtained experimental evidence that proves this [15]. The presence of P_{In} in LT InP was concluded from the ODMR studies by monitoring the photoluminescence (PL) and the MCDA. PL-ODMR signals indicate that the defect level at Ec-0.23 eV corresponds to the (+/++) charge transition of the P_{In} antisite [16]. An analysis of the free-carrier concentration as a function of the hydrostatic pressure showed the existence of a deep donor level at Ec+0.12 eV. Because the free electron concentration scales with the concentration of the P_{In}, determined by MCDA, as seen in Figure 7, this deep donor level is shown to correspond to the first ionization state (0/+) of the P antisite. We have sucessfully shown the the dominant deep donor level at Ec+0.12 eV in LT InP corresponds to the $P_{In}^{(0/+)}$. It is the autoionization of the P_{In} via its first ionization stage which leads to the n-type conductivity in as-grown LT InP. Thus we showed that the introduction of P_{In} in InP is not at all suitable to achieve SI material.

2.4. LT-InAlAs.

$In_{0.52}Al_{0.48}As$ is lattice matched to InP, so that it is very interesting to explore the properties of LT- $In_{0.52}Al_{0.48}As$ for application in InP-based devices. Previous work by Metzger et al. [17] gave evidence that (annealed) LT-InAlAs shows high resistivity, similar to LT-GaAs . In close collaboration with Dr. Metzger (then at Hughes Research Laboratories, Malibu), who provided the samples used in this study, we performed an extensive study of this material. Three types of structures were grown on semi-insulating InP substrates: LT-$In_{0.52}Al_{0.48}As$ directly grown at 250°C and annealed for 10min. at 490°C under As stabilization, $n^+ In_{0.52}Al_{0.48}As$ - LT-$In_{0.52}Al_{0.48}As$ - $p^+ In_{0.52}Al_{0.48}As$ structures, and $p^+ In_{0.52}Al_{0.48}As$ - LT-$In_{0.52}Al_{0.48}As$ - $n^+ In_{0.52}Al_{0.48}As$ structures. Due to the overgrowth of the doped layers at 490°C, all samples were annealed at this temperature. The first set of samples was used for Hall measurements, the other two sets for DLTS measurements after fabrication of mesa structures (Figure 8). Undoped and intentionally Be doped LT-$In_{0.52}Al_{0.48}As$ layers were used. Contrary to the previous results [17], Hall measurements of undoped LT-$In_{0.52}Al_{0.48}As$ revealed a resistivity of only 10^3 Ωcm. The discrepancy with the earlier results might be due to the fact that in the earlier work GaInAs contact layers were used, so that carrier transport had to cross heterointerfaces and interfacial barriers might have contributed to the high total resistance. The residual conductivity turned out to be due to a deep donor about 0.32-0.34eV below the conduction band edge. Be-doping obviously compensated this deep donor, so that resistivities of 3×10^4 Ωcm and 3×10^5 Ωcm were achieved for nominal Be doping levels of 10^{16} cm^{-3} and 10^{17} cm^{-3}, respectively. The corresponding positions of the Fermi energy are shown in Fig. 9 [18]. DLTS measurements confirmed the existence of deep traps in the upper half of the band gap; a representative spectrum and Arrhenius plot of the carrier emission rates are shown in Fig. 10 [18]. After correction for the capture barrier of about 30meV, the deep level activation energy turned out to be in the 0.40-0.45eV range. In view of the fact that the DLTS line showed strong line broadening (Fig. 10), the results of Hall effect and DLTS measurements might well be compatible. These results show that defects in the 0.3-0.4eV range below the conduction band prevented the formation of highly insulating, undoped LT-$In_{0.52}Al_{0.48}As$. In view of the results obtained for LT-InP, as described in the previous section, it is tempting to assign the donor-type defect levels in the upper half of the band gap to anion antisite defects, but a final determination, e.g., via magnetic resonance studies, could not be achieved in this case.

3. CONCLUSION.

We have studied native defects in various non-stoichiometric III-V semiconductor thin films using both optical and electrical characterization techniques. Results indicate that the anion antisite, As_{Ga}, dominates the properties of LT GaAs. This result allows future improvements in creating a highly

SI material compatible with GaAs for transistor fabrication. In LT-AlGaAs, the very deep arsenic antisite level permits the creation of layers with very high resistivity. In LT-InP and possibly in LT-InAlAs, the energy location of the anion antisite defects prevents the formation of highly resistive, undoped layers. With MCDA we could directly prove that LT InP is highly n-type due to P_{In} antisite defects and could try to resolve which transitions take place in the MCDA spectrum for this defect.

4. REFERENCES

1. J.M. Baranowski, Z. Liliental-Weber, W.-F. Yau, and E.R. Weber, *Phys. Rev. Lett.* **66**, 3079 (1991).

2. J.M. Baranowski, Z. Liliental-Weber, W.-F. Yau, and E.R. Weber, *Phys. Rev. Lett.* **68**, 551 (1992).

3. A. C. Warren, J. M. Woodall, J. L. Freeouf, D. Grischkowsky, D. T. McIntruff, M. R. Melloch, and N. Otsuka, *Appl. Phys. Lett.* **57**, 1331 (1990).

4. D. C. Look, D. C. Walters, M. O. Manasreh, J. R. Sizelove, C. E. Stutz, and K. R. Evans, *Phys. Rev.* **B 42**, 2578 (1990).

5. X. Liu, A. Prasad, W. M. Chen, A. Kurpiewski, A. Stoschek, Z. Liliental-Weber, and E. R. Weber, *Appl. Phys. Lett.* **65**, 3002 (1994).

6. Z. Liliental-Weber, J. Ager, D. Look, X. W. Lin, X. Liu, J. Nishio, K. Nichols, W, Schaff, W. Swider, K. Wang, J. Wasburn, E. R. Weber, and J. Whitaker, in: *"Semi-Insulating III-V Materials, Warsaw 1994"* Ed. M. Godlewski (World Scientific, Singapore 1994), p. 305

7. X. Liu, A. Prasad, J. Nishio, E. R. Weber, Z. Liliental-Weber, and W. Walukiewicz, *Appl. Phys. Lett.* **67**, 279 (1995).

8. S. B. Zhang and J. E. Northrup, *Phys. Rev. Lett.* **67**, 2339 (1991).

9. B. K. Meyer, J. M. Spaeth, and M. Scheffler, *Phys. Rev. Lett.* **52**, 851 (1984).

10. X. Liu, A. Prasad, W. M. Chen, and E. R. Weber, Proc. 22nd International Conference on the Physics of Semiconductors, ed. D. J. Lockwood (New Jersey, 1994), p. 2427.

11. P. J. Stephens, *Adv. Chem. Phys.* **35**, 197 (1976).

12. U. Kaufmann and J. Windscheif, *Phys. Rev.* **B 38**, 10060 (1988).

13. J. Menidez, A. Pinczuk, D. J. Werder, J. P. Valladares, T. H. Chiu, and W. T. Tsang, *Solid State Commun.* **61**, 703 (1987).

14. B. W. Liang, P. Z. Lee, D. W. Shih, and C. W. Tu, *Appl. Phys. Lett.* **60**, 2014 (1992).

15. W. M. Chen, P. Dreszer, A. Prasad, A. Kurpiewski, W. Walukiewicz, and E. R. Weber, *J. Appl. Phys.* **76**, 601 (1994).

16. W. M. Chen, P. Dreszer, E. R. Weber, E. Svrman, B. Monemar, B. W. Liang, and C. W. Tu, *J. Electron. Mater.* **22**, 1491 (1993).

17. R.A. Metzger , A. S. Brown, W. E. Stanchina, M. Lui, R. G. Wilson, T. V. Kargodorian, L. G. McCray and J. A. Henige, *J. Crystal Growth* 111, 445 (1991).

18. H.T. Chang, Masters Thesis, University of California, Berkeley 1994.

5. PUBLICATIONS

W. M. Chen, P. Dreszer, A. Prasad, A. Kurpiewski, W. Walukiewicz, and E. R. Weber, *J. Appl. Phys.* **76**, 600 (1994).

X. Liu, A. Prasad, W. M. Chen, A. Kurpiewski, A. Stoschek, Z. Liliental-Weber, and E. R. Weber, *Appl. Phys. Lett.* **65**, 3002 (1994).

X. Liu, A. Prasad, W. M. Chen, and E. R. Weber, 22nd International Conference on the Physics of Semiconductors, ed. D. J. Lockwood (New Jersey, 1994) 2427.

H. Fujioka, J. Krueger, A. Prasad, X. Liu, E. R. Weber and A. K. Verma, *J. Appl. Phys.* **78**, 1470 (1995).

X. Liu, A. Prasad, J. Nishio, E. R. Weber, Z. Liliental-Weber, and W. Walukiewicz, *Appl. Phys. Lett.* **67**, 279 (1995).

A. Prasad, X. Liu, P. Stallinga, and E. R. Weber, *Mats. Res. Soc. Symp. Proc.* 378 (1995).

A. Prasad, X. Liu, H. Fujioka, N. D. Jaeger, J. Nishio, and E. R Weber, Proc. 18th Internat. Conf. on Drfects in Semiconductors (Sendai 1995), in print.
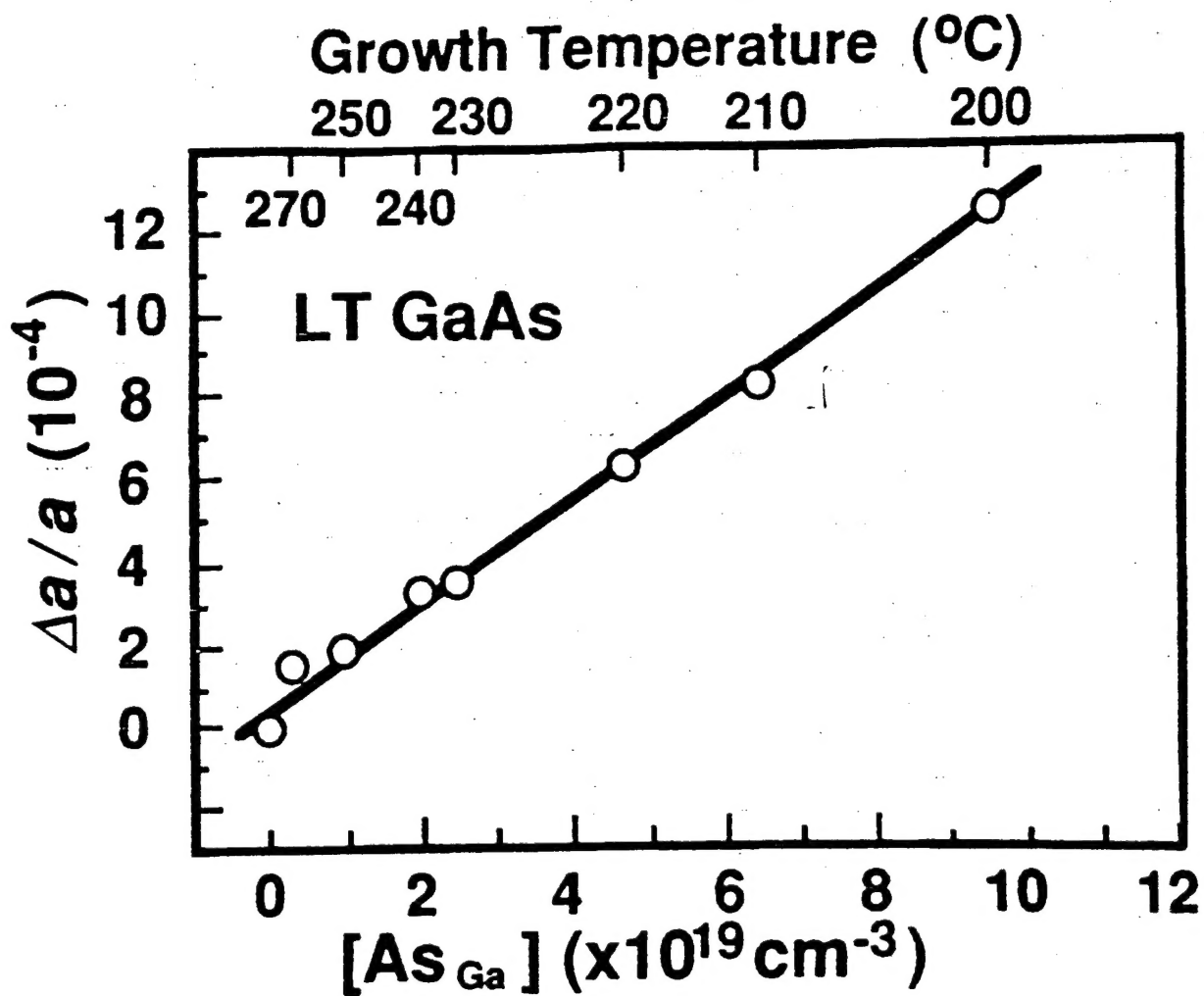
6. FIGURES
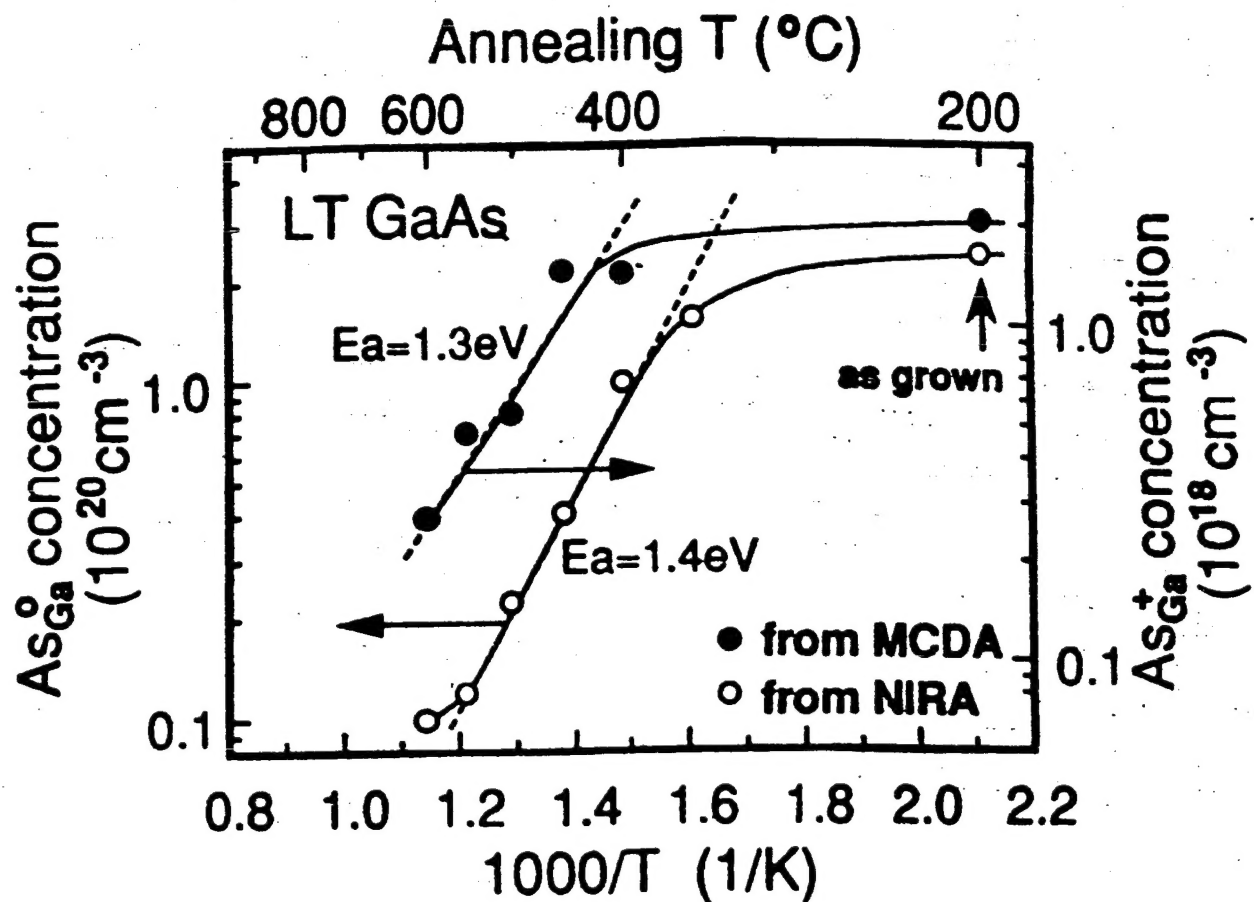
Annealing T (°C)

Figure 1: Concentration of As_{Ga}^0 and As_{Ga}^+, determined by NIRA and MCDA, respectively, as a function of the isochronal annealing temperature. The sample was grown on a semi-insulating substrate at 200°C.
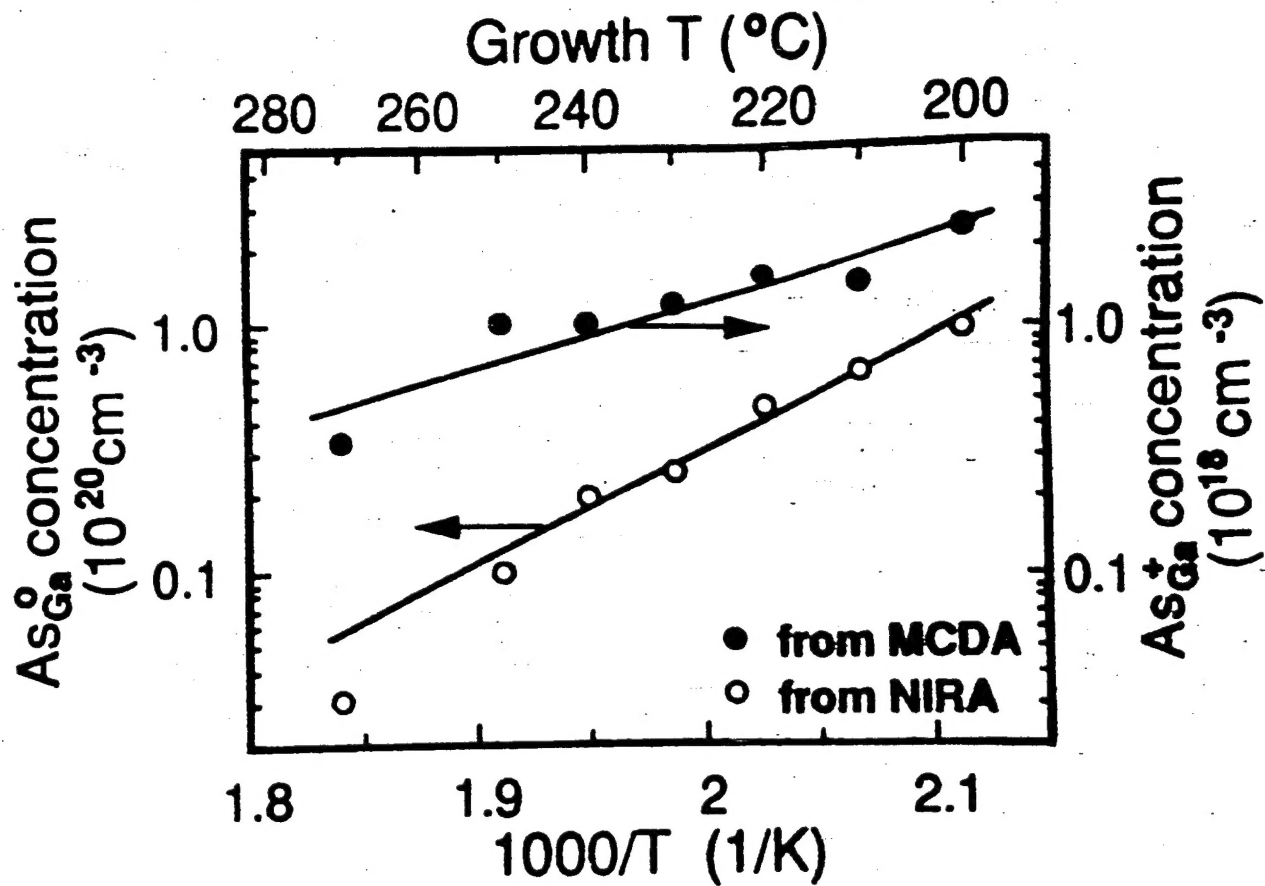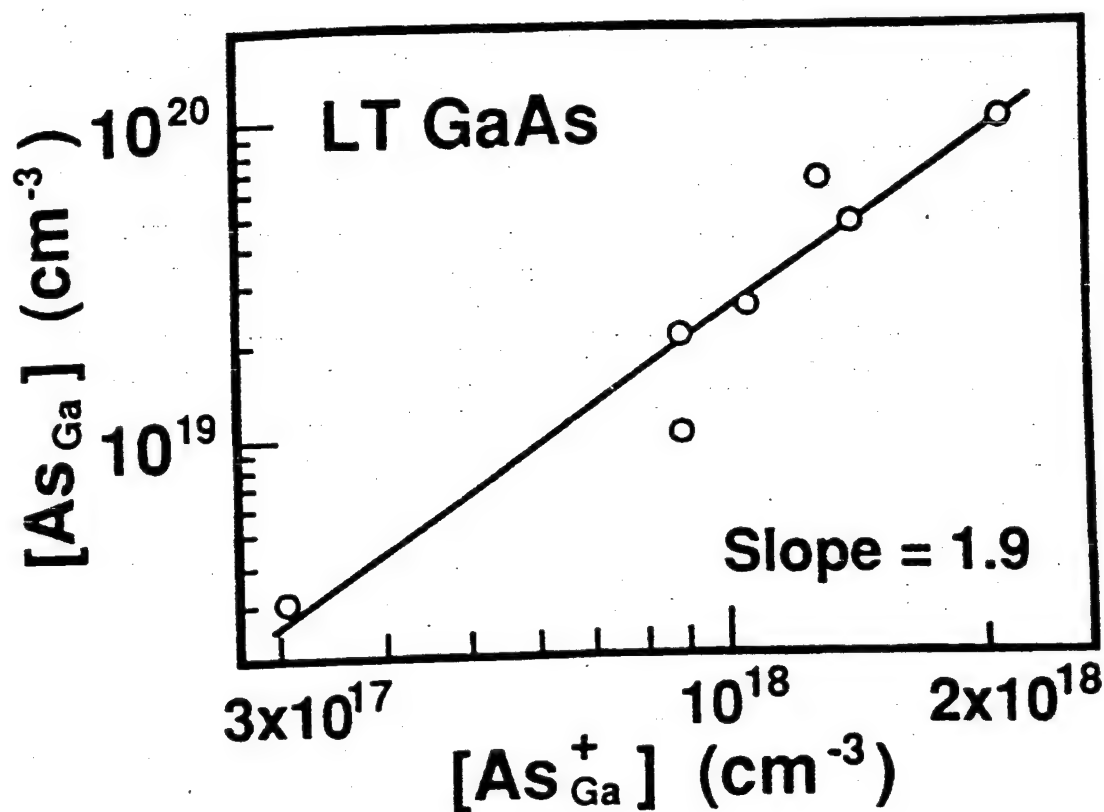
Figure 2: Concentration of As_{Ga}^0 and As_{Ga}^+, determined by NIRA and MCDA, respectively, as a function of the growth temperature. The samples were grown on SI substrates.

Figure 3: Relative change of lattice parameter plotted as a function of the concentration of As$_{Ga}$ for LT GaAs grown at different tempratures.

Figure 4: A log-log plot of the total concentration of antisites As_{Ga} as a function of the concentration of antisites As_{Ga} in the positively charged state. A near-second-power dependence of the two is observed.
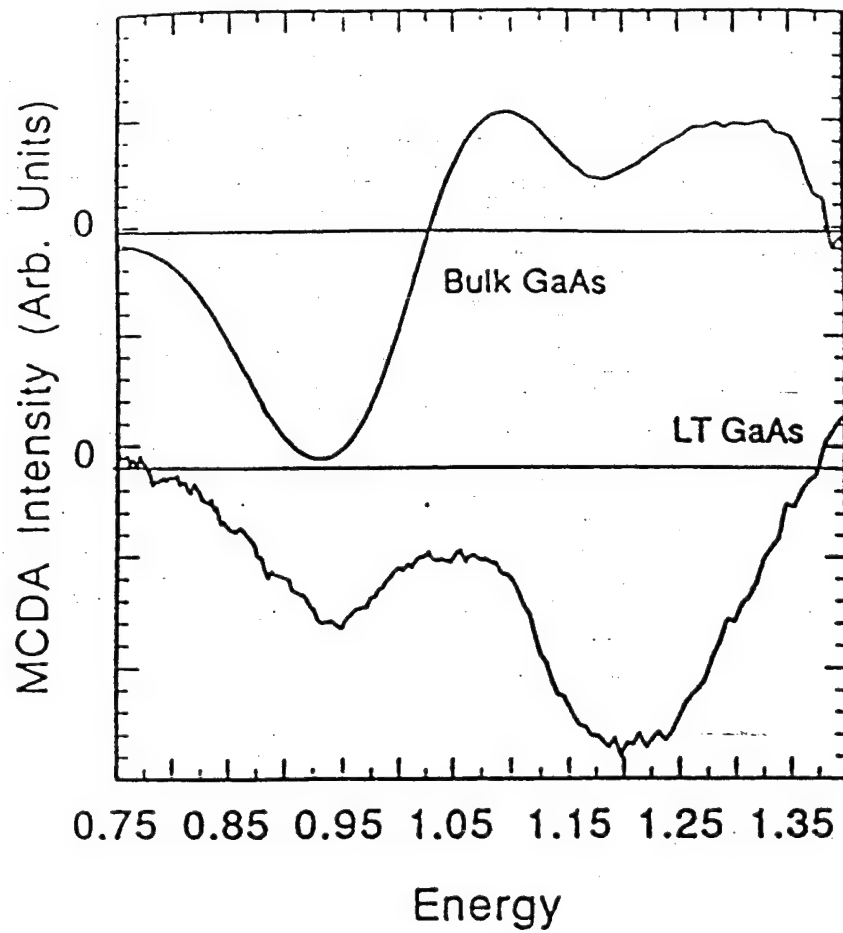
Figure 5: Typical MCDA spectra of As$_{Ga}$ defects in bulk SI GaAs and LT GaAs grown at 210°C. The spectra are measured at T=1.8K and B=2T.
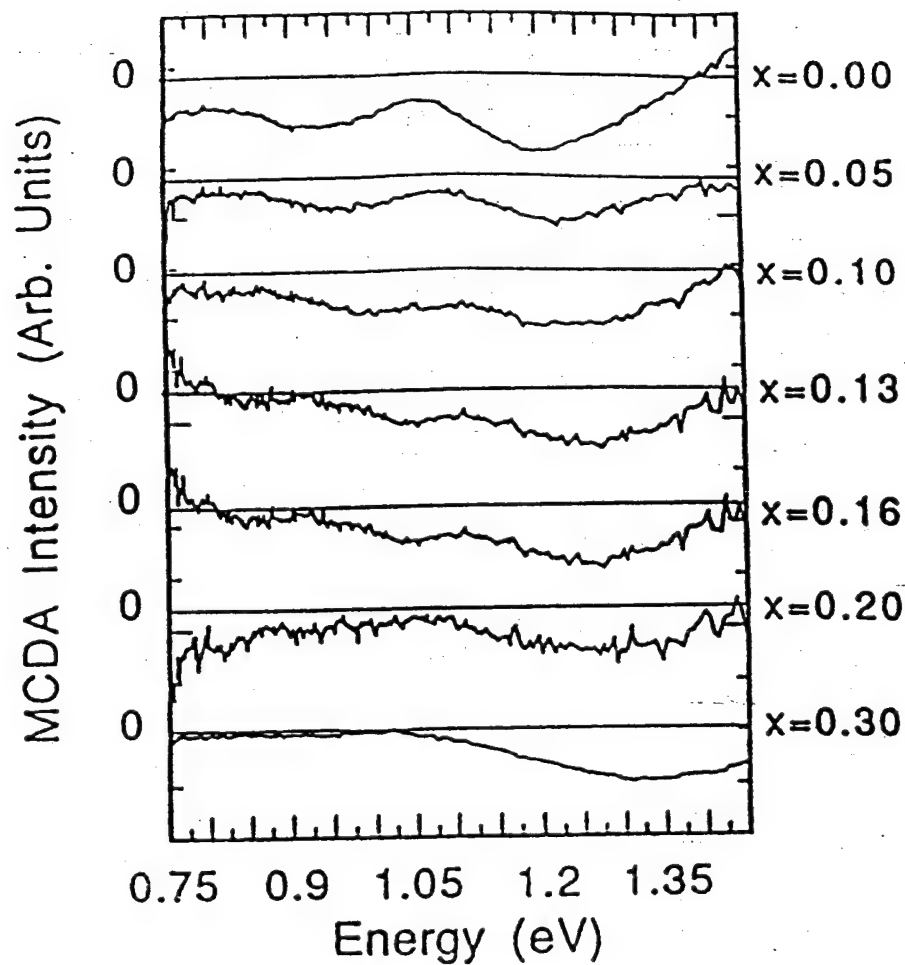
Figure 6: MCDA spectra of LT Al$_x$Ga$_{1-x}$As as a function of increasing Al content. The two negative peaks shift to higher energies with increasing x. The paramagnetic band starting at 0.94 eV shifts faster than the diamagnetic band at 1.18 eV for x=0.0, and eventually only the one peak is observable.
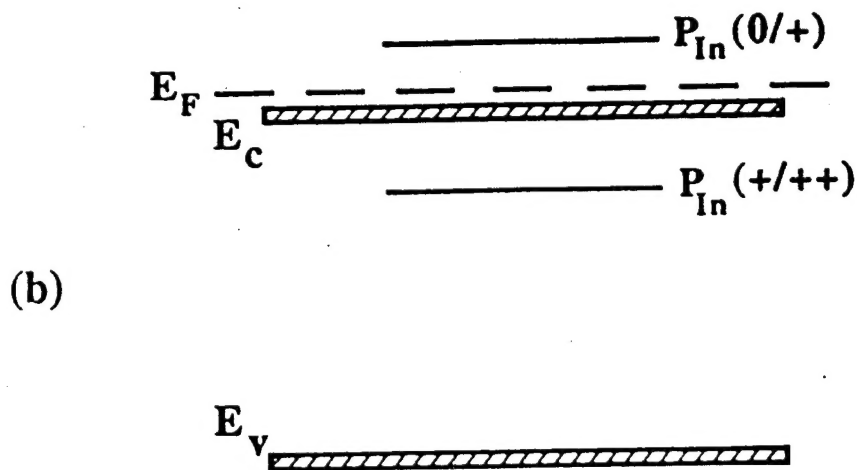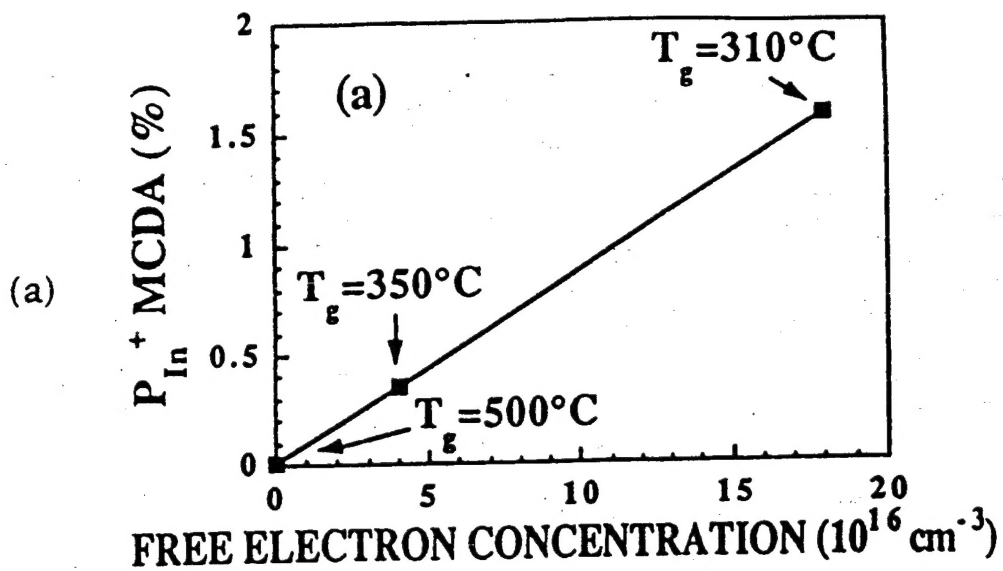
Figure 7: (a) Correlation between the free-electron concentration and MCDA intensity of the P_{In}^+ antisite in LT InP as a function of growth temperature T_g; (b) Energy-level scheme of the P_{In} antisite in LT InP.

Mesa Contacts
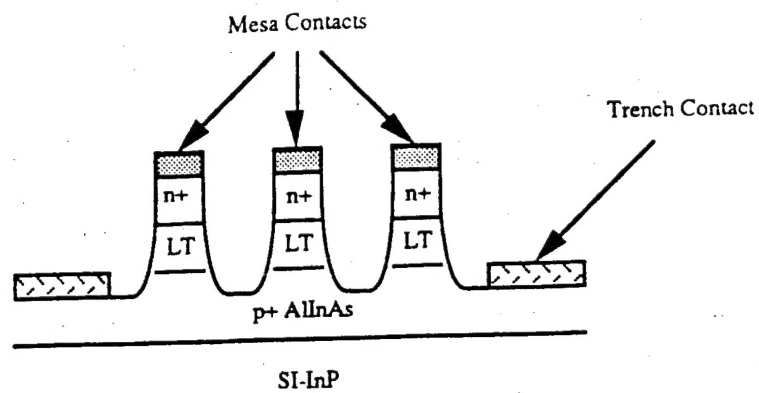
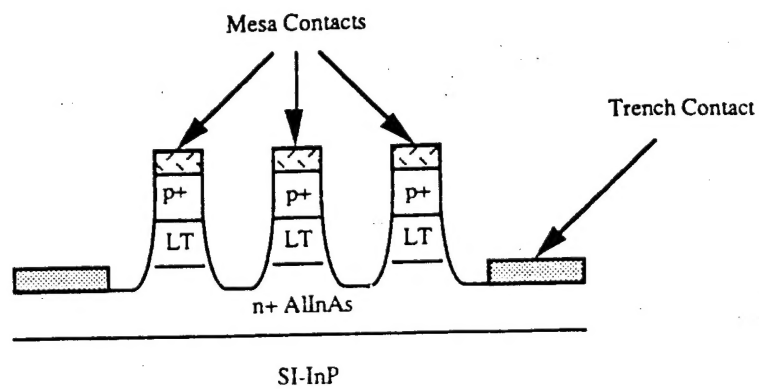Trench Contact

n+   n+   n+

LT   LT   LT

p+ AlInAs

SI-InP

Figure (a)

Mesa Contacts

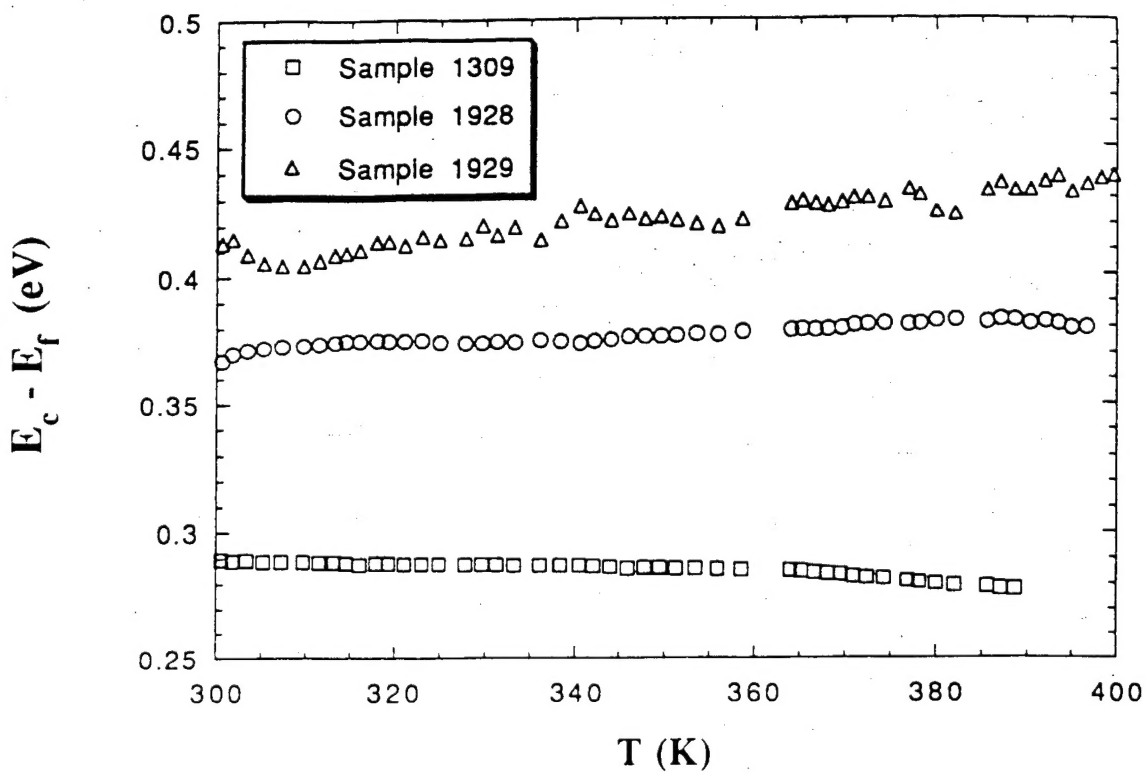Trench Contact

p+   p+   p+

LT   LT   LT

n+ AlInAs

SI-InP

Figure (b)

Figure 8: (a) n^+/n LT-AlInAs/p^+ diodes, with trench contacts made of Au-Zn and mesa contacts made of Au-Ge, and (b) p^+/p LT-AlInAs/n^+ diodes with trench contacts made of Au-Ge and mesa contacts made of Au-Zn.

Figure 9: Illustration of the Fermi level position, E_c-E_f, as a function of temperature for LT-AlInAs grown at 250°C. Sample 1309 is undoped, sample 1928 is doped with intended $p=10^{16}$ cm^{-3}, and sample 1929 is doped with intended $p=10^{17}$ cm^{-3}.
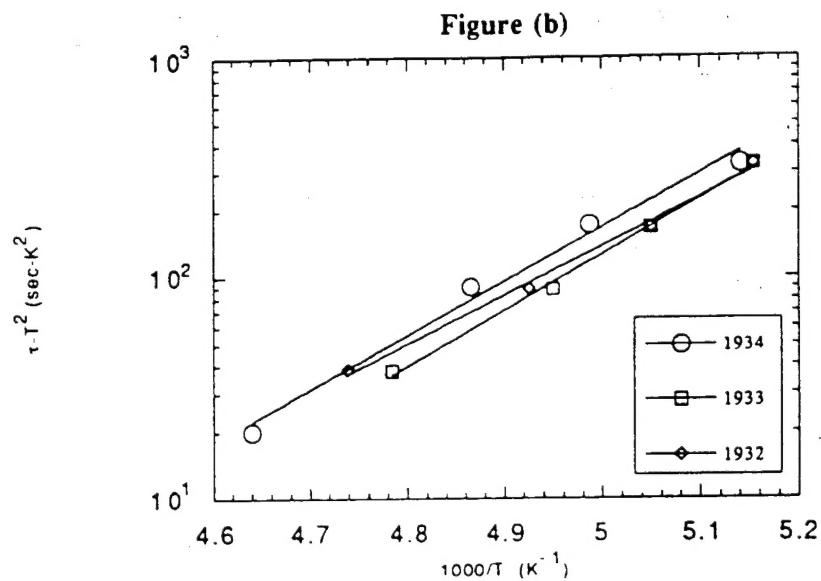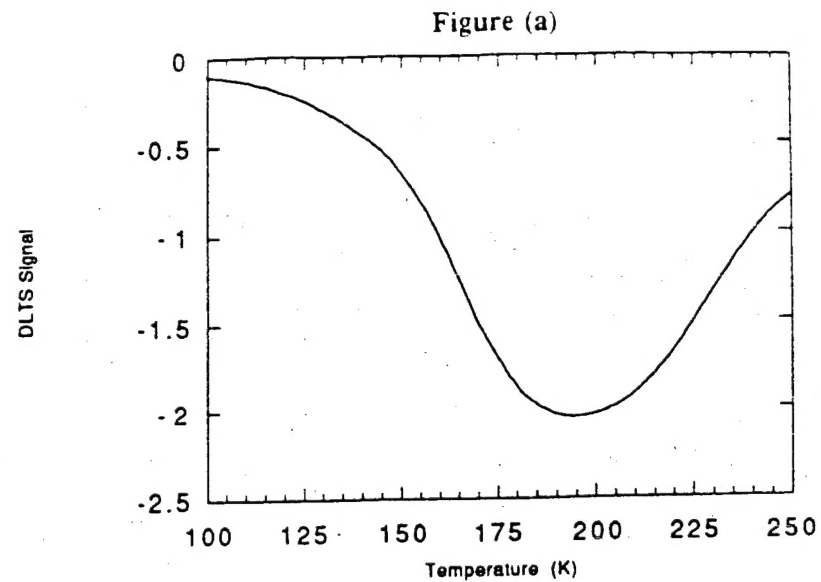
Figure (a)

Figure (b)

Figure 10: (a) DLTS spectra of sample 1934, identical in respect to the other LT-AlInAs samples, and (b) the temperature dependence of emission time constants τ for all the samples.